

# Cloud Based Image Contrast Enhancement

Shiqi Wang\*, Ke Gu<sup>†</sup>, Siwei Ma\*, Weisi Lin<sup>‡</sup>, Xiang Zhang\* and Wen Gao\*

\*School of Electronic Engineering & Computer Science, Peking Univ., Beijing, China, 100871

<sup>†</sup>Insti. of Image Commu. Infor. Proce., Shanghai Jiao Tong Univ., Shanghai, China, 200240

<sup>‡</sup>School of Computer Engineering, Nanyang Technological Univ., Singapore, 639798

**Abstract**—We propose a cloud based image contrast enhancement framework, in which the context-sensitive and context-free contrast is improved via solving a multi-criteria optimization problem. Specifically, the context-sensitive contrast enhancement is based on the unsharp masking of the input and edge-preserving filtered images, while the context-free contrast enhancement is achieved by the sigmoid transfer mapping. The parameters in the optimization process are determined with the reference to the image that has a similar content and better enhancement quality in the cloud. The image complexity from the free energy based brain theory and the “surface” quality statistics is collaboratively optimized to infer the parameters. Experimental results demonstrate that the proposed technique can efficiently create visually-pleasing enhanced images with the guidance image from cloud.

**Index Terms**—contrast enhancement, cloud image, unsharp masking, sigmoid transfer mapping

## I. INTRODUCTION

Contrast enhancement plays an important role in image processing and computer vision applications. Due to poor illumination conditions, low-quality, low-cost imaging sensors and users’ inexperience and operation errors, images and videos may not have proper visibility details for the captured scene. Contrast enhancement targets to eliminate these problems, and thereby produces a visually-pleasing and informative image.

To enhance the contrast and improve the visual quality, various post-processing algorithms have been proposed. Generally, these methods can be classified into two categories, the context-sensitive and context-free approaches [1]. The context-sensitive approach aims to enhance the local contrast that is dependent on the rate of change in intensity. It is noted that context-sensitive techniques are prone to artifacts such as noise and ringing, as enhancement of these undesirable details will very likely introduce annoying distortions [2]. Another branch of study is the context-free approach, which adopts a statistical method such as manipulating the pixel histogram. For example, in the well-known histogram modification (HM) framework, the gray-levels are spread to generate a more uniform distribution. Basically, the HM methods include histogram equalization (HE) [3] and its derivatives such as brightness preserving bi-histogram equalization (BBHE) [4], dualistic sub-Image histogram equalization (DSIHE) [5], recursive mean-separate histogram equalization (RMSHE) [6], recursive sub-image histogram equalization (RSIHE) [7], and histogram modification framework (HMF) [8]. Another HM technique, the sigmoid transfer based brightness preserving

(STBP) algorithm [9], was proposed to produce visually-pleasing enhanced image according to the close relationship between the third order statistic (skewness) and the surface quality [10].

A good contrast enhancement algorithm should highlight indiscernible image details properly and suppress visual artifacts simultaneously. In light of this, we propose an unified contrast enhancement framework based on differentiation of context-sensitive and context-free models, where context sensitive model tends to enhance the local contrast from the difference of neighbouring pixels, while the context-free approach modifies statistical pixel distributions regardless of the local properties. Regarding to contrast enhancement, the following issues are addressed: 1) balancing between the noise robustness and sharpness enhancement; 2) balancing between local and global contrast enhancement. To address these, we propose a multi-criteria optimization framework, in which the input image, unsharp masking of input and edge-preserving filtered images, and the sigmoid transform version are simultaneously considered in optimizing the enhanced image.

Another contribution of this paper is to automatically derive the contrast enhancement level from the image in cloud. The cloud is characterized by a large quantity of resources, storage and data [11]. Cloud based image processing has demonstrated its power in a variety of applications, such as image coding [12], deionising [13] and restoration [14]. Basically, in contrast enhancement it is difficult to choose the best parameters that will achieve visually-pleasing quality. The commonly-used manual parameter tuning is impractical for most applications as it is labor intensive and time-consuming, and more importantly, only automatic operations are feasible in many meaningful situations. We address this problem by taking advantages of the cloud. With the advance of cloud computing, a huge number of images are stored and easily accessed. In the cloud, there is a high probability of finding very similar images, which are captured at the same location at different view, angles and focal length. Some of these images may even get enhanced by a manual software with a good contrast. We investigate the automatical contrast estimation problem with the free energy based brain theory [15] and surface quality [10], which infer the enhancement level in the way of feature matching, and consequently the parameters in the proposed algorithm are tuned adaptively to achieve better visual quality.

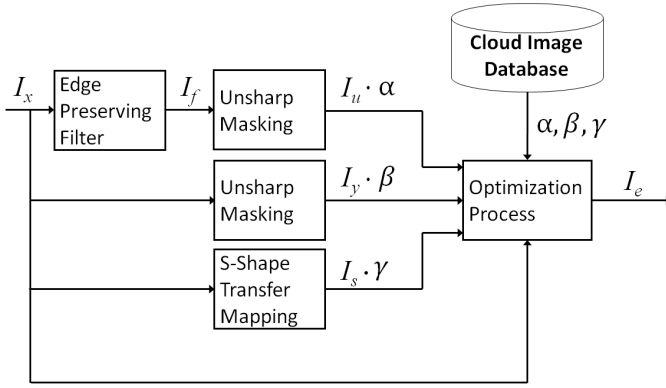


Fig. 1. Illustration of the unified contrast enhancement framework.

The remainder of this article is organized as follows. Section II presents the proposed unified framework for contrast enhancement. In Section III, we investigate the cloud based contrast enhancement level derivation. The effectiveness of our algorithm is demonstrated by comparison of its visual quality in Section IV. Finally, Section V concludes this paper.

## II. CONTRAST ENHANCEMENT FRAMEWORK

In this section, we demonstrate the unified contrast enhancement framework by leveraging the context-sensitive and context-free contrast enhancement methods. The advantages of these two approaches are incorporated with a combined strategy, which generates more visual-pleasing images. As illustrated in Fig. 1, the input image  $I_x$  is firstly filtered by an edge-preserving filter, which smooths away detailed textures while retaining sharp edges. The unsharp masking of the input and filtered images are systematically combined for context-sensitivity contrast enhancement. The high contrast images of similar content from cloud can adaptively estimate the control parameters,  $\alpha$ ,  $\beta$  and  $\gamma$ , while the final enhanced image  $I_e$  is produced with the determined parameters. More details of the proposed scheme will be discussed in the rest of this section.

### A. Context-Sensitive Approach

The unsharp masking is applied as the context-sensitive enhancement approach, which enhances the local contrast according to the rate of intensity change. The general framework of unsharp masking can be formulated as follows,

$$I_u = h(I'_x) + g(I_x - I'_x), \quad (1)$$

where  $I_x$  represents the input image and  $I'_x$  represents corresponding low-pass filtered (such as Gaussian smoothing) image. Both  $h$  and  $g$  can be defined as a linear or non-linear functions [2]. Here we define,

$$h(x) = x, \quad (2)$$

and

$$g(x) = \omega \cdot x, \quad (3)$$

where  $\omega$  is a control factor that determines the enhancement level.

In general, the output of the filtering process can be regarded as fitting a particular model to the input [16], and the residuals are represented as follows,

$$I_r = I_x - I'_x. \quad (4)$$

The residual signals represented by  $I_x - I'_x$  generally contain both detailed image structure and image noise, while only detailed image structure should be enhanced. This motivated us to firstly filter the image with an edge-preserving filter, following by an unsharp masking process. This leads to an edge enhanced image  $I_u$ , as illustrated in Fig. 1. In this paper, we apply the bilateral filter [17], as it possesses well edge-preserving ability, and is also easy to construct and calculate [18].

It is noted that only applying the edge-preserving filter would give rise to detailed information loss. In light of this, we perform unsharp masking to both the input image  $I_x$  and  $I_f$ . As such, the balance between the noise robustness and sharpness enhancement can be achieved.

### B. Context-Free Approach

The context-free component is from the recently proposed sigmoid transfer mapping [9]. The authors of [10] found that human eyes use skewness or a similar measure of histogram asymmetry in judging the surface quality, and an image with a long positive tail in histogram (namely a positively skewed statistics) tends to appear darker and glossier. This motivates the usage of the sigmoid mapping to improve the surface quality. The mapping function  $M_s(\cdot)$  and its associated enhanced image  $I_s$  are obtained by a four-parameter logistic function as follows,

$$I_s = M_s(I_x, \phi) = \frac{\phi_1 - \phi_2}{1 + \exp(-\frac{I_i - \phi_3}{\phi_4})} + \phi_2, \quad (5)$$

where  $\phi = \{\phi_1, \phi_2, \phi_3, \phi_4\}$  are parameters to be determined. To derive these parameters, four points denoted as  $(y_i, x_i)$ ,  $i = \{1, 2, 3, 4\}$  should be firstly fixed prior to the transfer process. Three fixed pairs are fixed as follows,  $(y_1, x_1) = (0, 0)$ ,  $(y_2, x_2) = (255, 255)$ , and  $(y_3, x_3) = (\frac{l_{\max}}{2}, \frac{l_{\max}}{2})$ , where  $l_{\max}$  is the maximum intensity value of the input image. Another pair  $(x_4, y_4)$  can be freely set up to control the shape. For example,  $x_4$  can be fixed as a certain number and  $y_4$  can be freely adjusted. The optimal control parameters  $\phi$  are obtained by searching for the optimized value via the minimization of the following objective function,

$$\phi_o = \arg \min_{\phi} \sum_{i=1}^4 |x_i - M_s(y_i, \phi)|. \quad (6)$$

Sigmoid mapping curves with different control parameters are illustrated in Fig. 2. After obtaining the optimal parameters  $\phi_o$ , the image can be enhanced as,

$$I_s = \max(\min(M_s(I_x, \phi_o), 255), 0), \quad (7)$$

where max and min operations are used to clip  $I_s$ 's pixel values into the range of  $[0, 255]$ .

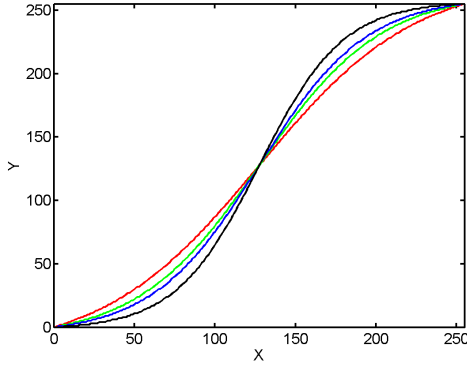


Fig. 2. Illustration of the sigmoid mapping.

### C. Unified Contrast Enhancement Framework

Both the context-sensitive and context-free approaches have their own advantages in optimizing the contrast quality, and therefore in this paper we formulate the contrast enhancement as a multi-criteria optimization problem. Basically, the goal is to find an image that is close to the enhanced images as desired, but also preserves the input image structure from  $I_x$ . Therefore, the general framework is defined as follows,

$$\min\{D(I_e - I_x) + \alpha \cdot D(I_e - I_u) + \beta \cdot D(I_e - I_y) + \gamma \cdot D(I_e - I_s)\}, \quad (8)$$

where  $\alpha$ ,  $\beta$  and  $\gamma$  are parameters that control the contrast enhancement level. Suppose  $\mathbf{x}$ ,  $\mathbf{y}$ ,  $\mathbf{e}$ ,  $\mathbf{f}$ ,  $\mathbf{u}$  and  $\mathbf{s}$  are the image signals for  $I_x$ ,  $I_y$ ,  $I_e$ ,  $I_f$ ,  $I_u$  and  $I_s$ , respectively. To obtain an analytical solution,  $D$  is defined as the squared sum of the Euclidean norm, which is formulated as follows,

$$D(\mathbf{x}, \mathbf{y}) = \sum_i (\mathbf{x}_i - \mathbf{y}_i)^2. \quad (9)$$

Combining Eqns. (8) and (9), the quadratic optimization problem is derived as follows,

$$\begin{aligned} \mathbf{e} &= \operatorname{argmin}_{\mathbf{e}} \{D(\mathbf{e}, \mathbf{x}) + \alpha \cdot D(\mathbf{e}, \mathbf{u}) + \\ &\quad \beta \cdot D(\mathbf{e}, \mathbf{y}) + \gamma \cdot D(\mathbf{e}, \mathbf{s})\} \\ &= \operatorname{argmin}_{\mathbf{e}} \{(\mathbf{e} - \mathbf{x})^T (\mathbf{e} - \mathbf{x}) + \alpha \cdot (\mathbf{e} - \mathbf{u})^T (\mathbf{e} - \mathbf{u}) \\ &\quad + \beta \cdot (\mathbf{e} - \mathbf{y})^T (\mathbf{e} - \mathbf{y}) + \gamma \cdot (\mathbf{e} - \mathbf{s})^T (\mathbf{e} - \mathbf{s}), \end{aligned} \quad (10)$$

resulting in,

$$\mathbf{e} = \frac{\mathbf{x} + \alpha \cdot \mathbf{u} + \beta \cdot \mathbf{y} + \gamma \cdot \mathbf{s}}{1 + \alpha + \beta + \gamma}. \quad (11)$$

Different  $\alpha$ ,  $\beta$  and  $\gamma$  will create different enhancement results. For example, when  $\gamma$  goes to infinity  $I_e$  converges to a global enhanced image, and when  $\alpha$ ,  $\beta$  and  $\gamma$  turns to zero,  $I_e$  preserves the input image. Therefore, various levels of contrast enhancement can be created by these three parameters.

In Fig. 3, we demonstrate the contrast enhancement results, including the input image, the HMF output [8], and the proposed scheme with  $\alpha = 0.5$ ,  $\beta = 0.5$  and  $\gamma = 0.5$ . It is

very obvious that the enhanced images produced by HMF can create visual artifacts. As the proposed scheme incorporates both the advantage of the context-free and context-sensitive approaches, it appears more visual-pleasing. In Fig. 3 (d)(e)(f), the middle enhanced image  $I_u$ ,  $I_y$ , and  $I_s$  are demonstrated. It is observed that the unsharp masking of the input image can preserve more details, but the undesired noise is introduced as well. While the unsharp masking of the filtered image only enhances the edge information, and detailed information is eliminated. Moreover, we observe that better surface quality is achieved with the sigmoid transfer in Fig. 2, as shown in Fig. 3 (f). As a matter of fact, the enhancement level is upper bounded by the image that has the highest contrast among  $I_u$ ,  $I_y$ , and  $I_s$ , and lower bounded by the input image  $I_x$ .

### III. CLOUD BASED CONTRAST ENHANCEMENT

In this section, an appropriate cloud image is used to help the contrast enhancement level derivation. Generally, a large number of near and partial duplicate images in the cloud are captured at the same location, but with different scale, orientation, and focus length. They have similar content as well as semantic meanings, and some of these images are post-processed to achieve better contrast and visual quality. For instance, 300 million photos are uploaded to Facebook every day. The images are captured with different devices and processed by different softwares, and many of them are correlated highly. A typical example is the landmark image, which is easy to be used to retrieve many highly correlated images in cloud [19]. In the following, the near duplicate image from cloud is also referred as the guidance image.

Generally, enhancing an image to a perfect contrast is difficult, as quality assessment of contrast enhancement is still a non-trivial task. Thanks to the availability of a large number of images from cloud, which make the automatical contrast enhancement possible. Here we make an assumption that some images from cloud have the perfect enhancement quality, as many of them are hand-picked and processed. The task is to derive the contrast enhancement level that best matches the guidance image. There are various methods for image matching. With registered image pairs, the image matching can be also formulated as a full image quality assessment problem to compute the distance between the image pairs. However, as the image from cloud may have different orientation and scale, it is difficult to directly apply a method here. Motivated by the design philosophy of reduced-reference image quality assessment [20], [21], features that can summary the whole image are extracted for matching. Moreover, in [22], [23] it is revealed that the image complexity and information is somehow related to the image quality, which motivated us to explore the contrast level derivation with recent findings on brain theory.

#### A. Free Energy Based Brain Theory

The free energy theory, which was recently introduced by Friston *et al.* in [15] and [24], tries to explain and unify several brain theories in biological and physical sciences about



Fig. 3. Comparison of the enhancement results. (a) Input image; (b) HMF output; (c) Proposed scheme with  $\alpha = 0.5$ ,  $\beta = 0.5$  and  $\gamma = 0.5$ ; (d)  $I_u$ ; (e)  $I_y$ ; (f)  $I_s$ .

human action, perception and learning. The basic premise of the free energy based brain theory is that the cognitive process is manipulated by an internal generative model (IGM). The human brain can actively infer predictions of the meaningful information of input visual signals and avoid the residual uncertainty in a constructive manner.

Assuming that the internal generative model  $\mathcal{M}$  for visual perception is parametric based, and this implies that the human brain perceives scenes by adjusting the parameter vector  $\mathbf{v}$ . Given an input image  $I$ , its ‘surprise’ (determined by entropy) is evaluated by integrating the joint distribution  $P(I, \mathbf{v})$  over the space of model parameters  $\mathbf{v}$

$$-\log P(I) = -\log \int P(I, \mathbf{v}) d\mathbf{v}. \quad (12)$$

A dummy term  $Q(\mathbf{v}|I)$  is integrated into both the denominator and numerator in Eq. (12), which can be rewritten as follows,

$$-\log P(I) = -\log \int Q(\mathbf{v}|I) \frac{P(I, \mathbf{v})}{Q(\mathbf{v}|I)} d\mathbf{v}, \quad (13)$$

where  $Q(\mathbf{v}|I)$  is an posterior distribution of the model parameters given the input image signal  $I$ . This can be regarded as the posterior approximation to the true posterior of the model parameters  $P(\mathbf{v}|I)$  in the cognitive process. Another interpretation is that when we perceives the image  $I$  or when adjusting the parameters  $\mathbf{v}$  of  $Q(\mathbf{v}|I)$  to search for the optimal explanation of  $I$ , the brain will minimize the discrepancy between the approximate posterior  $Q(\mathbf{v}|I)$  and the true posterior  $P(\mathbf{v}|I)$ .

By applying Jensen’s inequality, from Eqn. (13) we derive

that,

$$-\log P(I) \leq -\int Q(\mathbf{v}|I) \log \frac{P(I, \mathbf{v})}{Q(\mathbf{v}|I)} d\mathbf{v}, \quad (14)$$

and the free energy is defined as follows,

$$\mathcal{F}(\mathbf{v}) = -\int Q(\mathbf{v}|I) \log \frac{P(I, \mathbf{v})}{Q(\mathbf{v}|I)} d\mathbf{v}. \quad (15)$$

The free energy based brain theory reveals that the human visual system (HVS) cannot fully process all of the sensation information and tries to avoid some surprises with uncertainties, and these uncertainties can be regarded as free-energy. In [25], the free energy is approximated to be the entropy of prediction residuals plus the model cost. In practice, positive contrast change renders high quality images by highlighting the visibility details, which produces more informative content. When perceiving the positive contrast image, the additional informative content will make the image more difficult to describe, as in general the HVS has stronger description ability for low-complexity images than high-complexity versions. The prior information in the cloud is able to predict the appropriate free energy of a visual-pleasing image with a good contrast, which is very efficient in deriving the contrast enhancement levels.

In practice, being aware of the computational complexity issue, in this work the free energy is characterized by the entropy of residuals after low-pass filtering [25]. For an image  $I_c$  from the cloud, it is defined as follows,

$$\mathcal{C}(I_c) = E(I_c - I'_c), \quad (16)$$

where  $E$  denotes the entropy function.

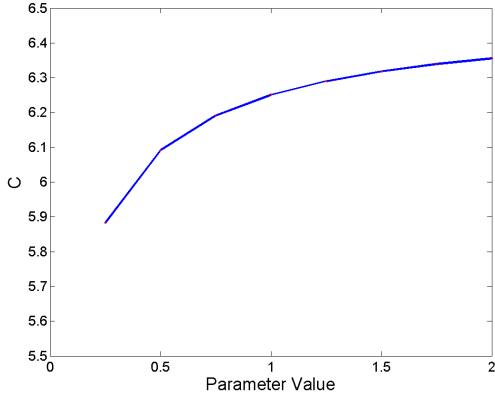


Fig. 4. The relation between the parameter value and  $C$ .

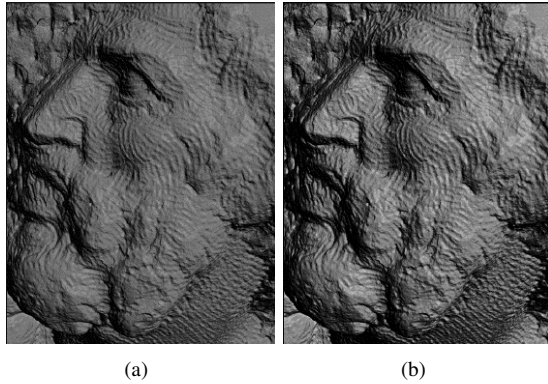


Fig. 5. Surface quality comparison of two synthetic images of Michelangelo's St Matthew sculpture with the same mean luminance [10]. (a) skewness: -0.62; (b) skewness: -0.13.

The relationship between the contrast enhancement level and  $C$  is demonstrated in Fig. 4. It is noted that  $\alpha = \beta = \gamma$  and these parameters are represented by the x-axis. It is observed that the free-energy  $C$  is increasing monotonously with the contrast level, which indicates that it has strong description ability for contrast. Moreover, it is noted that  $C$  is bounded by the enhanced image with the highest contrast, as discussed in last paragraph of Section II-C.

### B. Surface Quality Statistics

In [10], it is discovered that the human observers use skewness, or histogram asymmetry to judge the surface quality. In Fig. 5, it is observed that the right image appears darker and glossier than the left one, and moreover, the skewness of the left image is lower than the right one. Skewness is a measure of the asymmetry of a distribution; and it indicates the balance between the positive and negative tails. Furthermore, a possible neural mechanism was proposed to explain the skewness from physiology in human brains, which includes on-center and off-center cells and an accelerating nonlinearity to compute the subband skewness.

### C. Contrast Level Derivation From Cloud

Based on the analysis of free-energy and surface quality statistics, two features are extracted from the cloud image to guide the contrast level derivation. Instead of pixel-wisely or patch-wisely comparing image pairs, two global features achieve high efficiency in dimension reduction, and also provide good accuracy in summarizing the contrast strength. Therefore, contrast matching can be converted to the optimization problem based on the cloud image  $I_c$  and the enhanced image  $I_e$  as follows,

$$\min \|C(I_c) - C(I_e)\| + \lambda \|S(I_c) - S(I_e)\|, \quad (17)$$

where the function  $S$  represents the skewness of the input image, and parameter  $\lambda$  balances the magnitude and importance between the complexity measure and skewness measure. Referring to the optimal value in the optimization process of Eqn. (17) as  $L(I_c, I_e)$ , finding the parameters is based on solving,

$$(\alpha^*, \beta^*, \gamma^*) = \arg \min_{\alpha, \beta, \gamma} L(I_c, I_e). \quad (18)$$

Practically, as context-sensitive contrast is increasing monotonously with the image complexity, and the context-free contrast increases with the surface quality, we perform a simpler search to obtain the best enhancement level, which first performs a grid search in a given range of parameters followed by a binary search within the reduced ranges.

## IV. EXPERIMENTAL RESULTS

In this section, experiments are conducted to verify the proposed cloud based contrast enhancement scheme. To be general, images from the Berkeley database [26] are used for comparison, and traditional HE and the popular HM methods [8] are used for comparison to demonstrate the effectiveness of the proposed technique. The guidance images from the database are firstly manually enhanced to an appropriate level to examine the scheme. In Figs. 6-9, the guidance images, the enhanced guidance images by subjects, the input image and the images that are automatically enhanced by the proposed scheme are demonstrated.

As given in Figs. 6-9 (c), the HE produces excessively enhanced unnatural looking images. This results from the large backward-difference of the equalized histogram. Though HMF targets at solving this problem, it is lack of enhancing the details, such as the bottom of Fig. 8 (f). Moreover, as shown in Fig. 7 (f), the HMF output produces clearly artifacts. In comparison, our model not only appropriately enhances the detailed information, but also generates much glossier images, being enabled by the sigmoid transfer mapping.

Though our scheme blindly estimates the contrast level by matching the features of the guidance image, the enhancement level of our scheme can well match that of the guidance image. Moreover, it is noted that in this experiment, a guidance image is captured not only at a similar location, but also with different content (just with similar semantic information), such as in Fig. 7.



Fig. 6. Results comparison. (a) Guidance image; (b) Enhanced guidance image; (c) HE output; (d) Input image; (e) Enhanced image; (f) HMF output.



Fig. 7. Results comparison. (a) Guidance image; (b) Enhanced guidance image; (c) HE output; (d) Input image; (e) Enhanced image; (f) HMF output.

## V. CONCLUSION

The novelty of this paper lies in that we propose a unified framework by leveraging the context-sensitivity and context-free contrast enhancement methods, and automatically choosing the enhancement degree with the guidance of the matched cloud image. The optimization problem is formulated as generating an image that is close to the input, local contrast enhanced, as well as the global contrast enhanced images.

In particular, with the utility of the cloud image, the blind estimation process of the contrast enhancement level is proposed based on the theory of free-energy principle and surface quality. Experimental results demonstrate the effectiveness of the scheme in image enhancement applications.

## VI. ACKNOWLEDGEMENTS

This work was supported in part by the Major State Basic Research Development Program of China (2015CB351800)

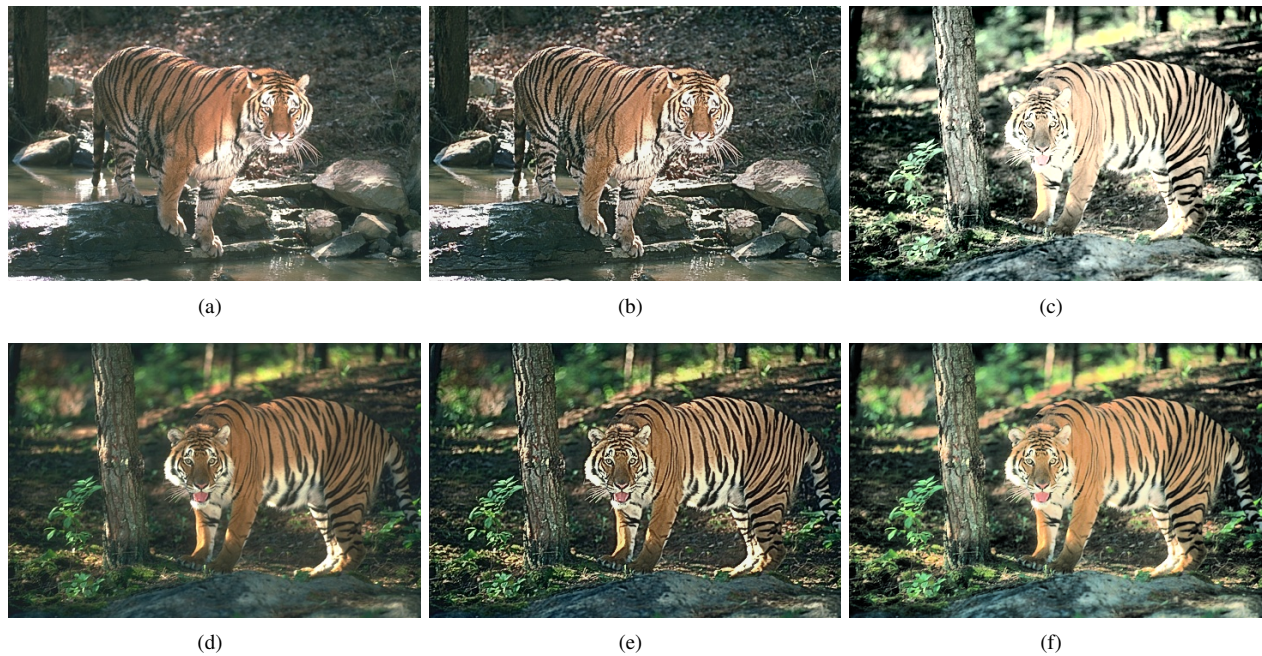


Fig. 8. Results comparison. (a) Guidance image; (b) Enhanced guidance image; (c) HE output; (d) Input image; (e) Enhanced image; (f) HMF output.

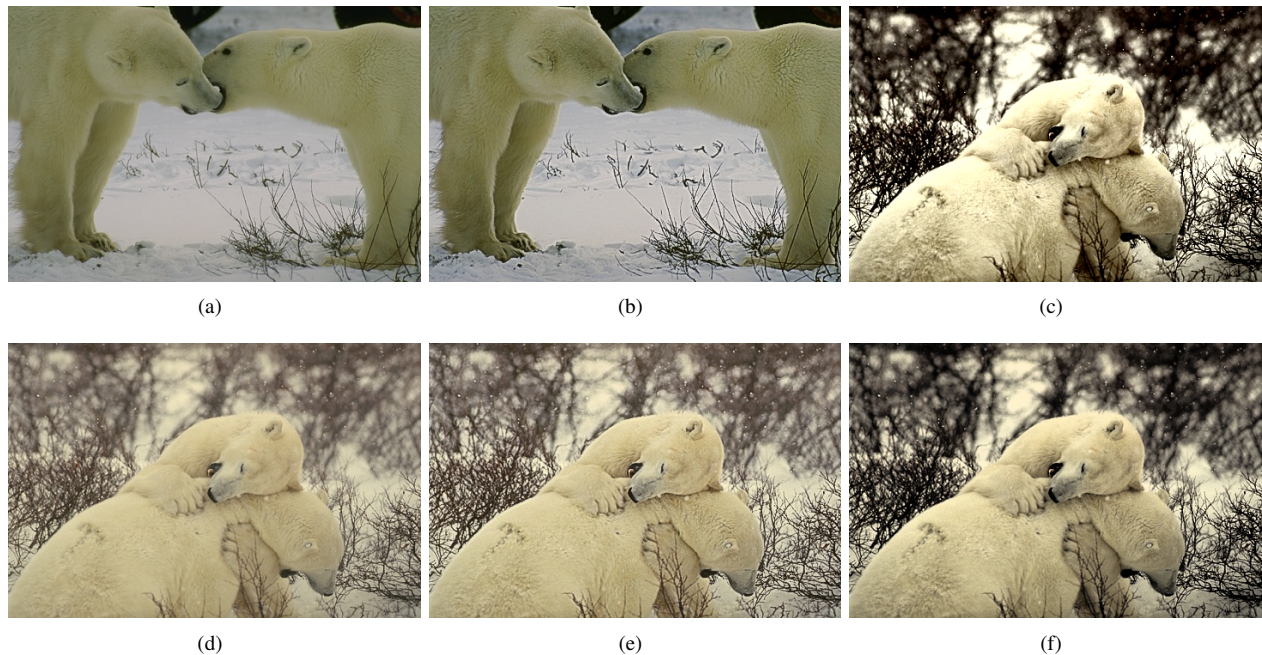


Fig. 9. Results comparison. (a) Guidance image; (b) Enhanced guidance image; (c) HE output; (d) Input image; (e) Enhanced image; (f) HMF output.

and in part by the National Science Foundation (61322106, 61390515 and 61210005). This work was also granted by Cooperative Medianet Innovation Center.

#### REFERENCES

- [1] Xiaolin Wu, "A linear programming approach for optimal contrast-tone mapping," *Image Processing, IEEE Transactions on*, vol. 20, no. 5, pp. 1262–1272, 2011.
- [2] Guang Deng, "A generalized unsharp masking algorithm," *Image Processing, IEEE Transactions on*, vol. 20, no. 5, pp. 1249–1261, 2011.
- [3] Rafael C Gonzalez and Richard E Woods, "Digital image processing," 2002.
- [4] Yeong-Taeg Kim, "Contrast enhancement using brightness preserving bi-histogram equalization," *Consumer Electronics, IEEE Transactions on*, vol. 43, no. 1, pp. 1–8, 1997.
- [5] Yu Wang, Qian Chen, and Baomin Zhang, "Image enhancement based on equal area dualistic sub-image histogram equalization method," *Consumer Electronics, IEEE Transactions on*, vol. 45, no. 1, pp. 68–75, 1999.
- [6] Soong-Der Chen and Abd Rahman Ramli, "Contrast enhancement using recursive mean-separate histogram equalization for scalable brightness

- preservation,” *Consumer Electronics, IEEE Transactions on*, vol. 49, no. 4, pp. 1301–1309, 2003.
- [7] KS Sim, CP Tso, and YY Tan, “Recursive sub-image histogram equalization applied to gray scale images,” *Pattern Recognition Letters*, vol. 28, no. 10, pp. 1209–1221, 2007.
  - [8] Tarik Arici, Salih Dikbas, and Yucel Altunbasak, “A histogram modification framework and its application for image contrast enhancement,” *Image Processing, IEEE Transactions on*, vol. 18, no. 9, pp. 1921–1935, 2009.
  - [9] Ke Gu, Guangtao Zhai, Min Liu, Xionghuo Min, Xiaokang Yang, and Wenjun Zhang, “Brightness preserving video contrast enhancement using s-shaped transfer function,” in *Visual Communications and Image Processing (VCIP), 2013*. IEEE, 2013, pp. 1–6.
  - [10] Isamu Motoyoshi, Shin’ya Nishida, Lavanya Sharan, and Edward H Adelson, “Image statistics and the perception of surface qualities,” *Nature*, vol. 447, no. 7141, pp. 206–209, 2007.
  - [11] Michael Armbrust, Armando Fox, Rean Griffith, Anthony D Joseph, Randy Katz, Andy Konwinski, Gunho Lee, David Patterson, Ariel Rabkin, Ion Stoica, et al., “A view of cloud computing,” *Communications of the ACM*, vol. 53, no. 4, pp. 50–58, 2010.
  - [12] Huanjing Yue, Xiaoyan Sun, Jingyu Yang, Feng Wu, et al., “Cloud-based image coding for mobile devices-toward thousands to one compression,” *IEEE Transactions on Multimedia*, vol. 15, no. 4, pp. 845–857, 2013.
  - [13] Huanjing Yue, Xiaoyan Sun, Jingyu Yang, and Feng Wu, “Cid: Combined image denoising in spatial and frequency domains using web images,” in *Computer Vision and Pattern Recognition (CVPR), 2014 IEEE Conference on*. IEEE, 2014, pp. 2933–2940.
  - [14] E Hung, D Garcia, and R De Queiroz, “Example-based enhancement of degraded video,” 2014.
  - [15] Karl Friston, “The free-energy principle: a unified brain theory?,” *Nature Reviews Neuroscience*, vol. 11, no. 2, pp. 127–138, 2010.
  - [16] John W Tukey, “Exploratory data analysis,” 1977.
  - [17] Carlo Tomasi and Roberto Manduchi, “Bilateral filtering for gray and color images,” in *Computer Vision, 1998. Sixth International Conference on*. IEEE, 1998, pp. 839–846.
  - [18] Peyman Milanfar, “A tour of modern image filtering,” *IEEE Signal Processing Magazine*, vol. 2, 2011.
  - [19] Huanjing Yue, Xiaoyan Sun, Jingyu Yang, and Feng Wu, “Landmark image super-resolution by retrieving web images,” 2013.
  - [20] Shiqi Wang, Xiang Zhang, Siwei Ma, and Wen Gao, “Reduced reference image quality assessment using entropy of primitives,” in *PCS*, 2013, pp. 193–196.
  - [21] Zhou Wang and Alan C Bovik, “Reduced-and no-reference image quality assessment,” *Signal Processing Magazine, IEEE*, vol. 28, no. 6, pp. 29–40, 2011.
  - [22] Xiang Zhang, Shiqi Wang, Siwei Ma, Shaohui Liu, and Wen Gao, “Entropy of primitive: A top-down methodology for evaluating the perceptual visual information,” in *Visual Communications and Image Processing (VCIP), 2013*. IEEE, 2013.
  - [23] Xiang Zhang, Shiqi Wang, Siwei Ma, Ruiqin Xiong, and Wen Gao, “Towards accurate visual information estimation with entropy of primitive,” in *IEEE International Symposium on Circuits and Systems (ISCAS)*. IEEE, 2015.
  - [24] Karl Friston, James Kilner, and Lee Harrison, “A free energy principle for the brain,” *Journal of Physiology-Paris*, vol. 100, no. 1, pp. 70–87, 2006.
  - [25] Guangtao Zhai, Xiaolin Wu, Xiaokang Yang, Weisi Lin, and Wenjun Zhang, “A psychovisual quality metric in free-energy principle,” *Image Processing, IEEE Transactions on*, vol. 21, no. 1, pp. 41–52, 2012.
  - [26] David Martin, Charless Fowlkes, Doron Tal, and Jitendra Malik, “A database of human segmented natural images and its application to evaluating segmentation algorithms and measuring ecological statistics,” in *Computer Vision, 2001. ICCV 2001. Proceedings. Eighth IEEE International Conference on*. IEEE, 2001, vol. 2, pp. 416–423.